An Implantable Drug Delivery Device based on MEMS Technology for Treatment of Hemorrhagic Shock on the Battlefield

N. M. Elman*, H-L Ho Duc* and M. J. Cima*
*Massachusetts Institute of Technology, Department of Materials Science and Engineering
Room 12-011, Cambridge 02139, USA, nelman@mit.edu

ABSTRACT

A novel drug delivery system based on MEMS (Micro-Electro-Mechanical-Systems) technology was developed for the immediate treatment of hemorrhagic shock of soldiers affected on the battlefield. A miniaturized drug delivery system was developed and implemented as an implantable biochip capable of delivering vasopressin *in vivo*, a known vasoconstrictor, in 0.02-0.1 ml volumes. Such implantable biochip was specially tailored to treat hemorrhagic shock in ambulatory settings. The biochip MEMS design allows controlled release of the drug. The biochip design is intended for *in vivo* use as a micro-implant in the peritoneum. We believe that the ramifications of this new MEMS-based drug delivery system can also be applicable to a vast number of medical applications for civilian use.

Keywords: MEMS, Drug delivery, Micro-implant, Biochip

1 INTRODUCTION

Hemorrhagic shock is treated in hospital settings by a combination of hemorrhage control, fluid replacement and the injection of vasoconstrictor agents, such as epinephrine. Hemorrhagic shock is characterized by a hypotensive state of deficient organ perfusion caused by blood loss from extremity wounds or internal injuries [1]. Battlefield conditions, however, impede the timely administration of these measures as in many occasions, paramedics may be prevented from treating wounded soldiers on site. Therefore, conditions in the battlefield demand for real-time treatment of hemorrhagic shock of soldiers in ambulatory settings. We present in this work a novel implantable drug delivery device designed to deliver the known vasoconstrictor vasopressin *in vivo*. The device was designed to be preemptively implanted in soldiers exposed to high risk scenarios. We present the device design, fabrication process, and preliminary experimental results.

2 DEVICE DESCRIPTION

The drug delivery device consists of three layers: a large reservoir layer, where the drugs are stored, a membrane layer from where the drug is ejected, and a bubble generator layer, where bubbles are formed. Figure 1 shows the overall system. The bubble generator layer consists of patterned metal electrodes that can be electrically configured to act as either heating elements (resistors), or parallel electrodes. Bubbles can therefore be formed using either configuration. Vapor bubbles form by means of film boiling or nucleate boiling, as a voltage is applied across the arrays of resistors in the first configuration [2]. The second configuration forms bubbles by hydrolysis, where water molecules are separated into hydrogen and oxygen [3]. The local phase transition to gas close to the surface of the resistors serves to break the SiN membranes and eject the liquid at a high flow rate. Gold fuses defined on top of the SiN membranes are designed to act as sensors: if a specific membrane is burst, the electrical connection will be disrupted and it will therefore be possible to determine whether and which of the membranes was burst by checking for electrical impedance.

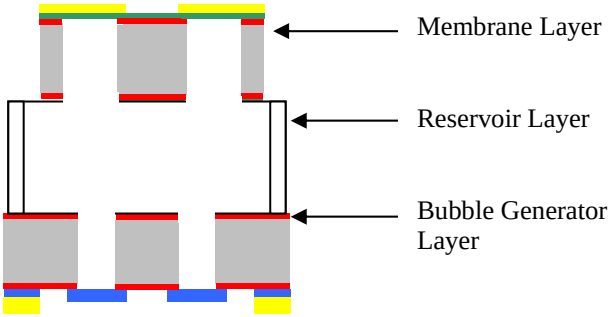

Figure 1: Cross-section of device composed of the three layers

3 FABRICATION

Each of the described layers was fabricated independently using a separate fabrication process. The glass layer consisted of a 100-mm Pyrex 7740 wafer, 2.2 mm thick, which was first drilled through using a 2 mm diameter diamond drilling bit in order to define the dimensions of the reservoir.

The membrane layer was fabricated using micro-machining technology. The process sequence is illustrated in Figure 3. The first step is to grow a 500 nm thermal silicon dioxide (SiO_2) layer on a 100-mm, double polished, 300-μm thick, single-crystal-silicon (SCS) wafer. A 200-nm layer of SiN is subsequently deposited using low-pressure vapor chemical deposition (LPCVD), shown in Fig. 2A. Next, a 50 nm Ti layer followed by a 300 nm gold

NSTI-Nanotech 2007, www.nsti.org, ISBN 1420061836 Vol. 2, 2007

layer are sputtered. The first photolithographic step follows, to define the electrical fuses that are laid out on top of the membranes to be defined, shown in Fig. 2B. A thin layer of photoresist is patterned on the gold layer, and Au and Ti etches follow, patterning the fuses. The patterned wafer is then coated with a layer of photoresist for protection. Next, the backside of the wafer is patterned to define the membranes, using a second photolithographic process, followed by CF_4-based reactive ion etch (RIE) to transfer the pattern to the backside SiO_2 and SiN layers. A deep RIE based on the Bosch^{tm} process is then performed to anisotropically etch through the wafer up to the silicon front-side buried SiO_2 layer, shown in Fig. 2C. Such layer acts as stop mask, and allows compensation for the 10 percent etch non-uniformity. The wafer is finally subjected to a 2-minute, 49 percent HF dip in order to remove the remaining oxide layer, shown in Fig. 2D.

The bubble generator layer was also fabricated using micro-machining technology. The process sequence is shown in Figure 3. The first step is to grow a 500 nm thermal SiO_2 layer. Next, a 200 nm Ta layer followed by a 200 nm Au layer are sputtered, shown in Fig. 3A. The first photolithographic process follows to pattern Au electrical contacts, shown in Fig. 3B. This step is followed by an Au etch. The second photolithographic step defines the Ta electrodes (serpentine topology), which are also wet etched, shown in Fig. 3C. The front side of the wafer is then coated with photoresist for protection. Next, the backside of the wafer is patterned using the third photolithographic step, followed by a CF_4-based RIE to transfer the pattern to the SiO_2 and SiN layers. The wafer is subsequently anisotropically etched through to the front-side buried SiO_2 layer, using the Bosch^{tm} process again, shown in Fig. 3D. The wafer is finally subjected to a CF_4-based RIE for etching the remaining buried SiO_2 and exposing the Ta resistors, shown in Fig. 3E.

Figure 2: Fabrication sequence for the membrane layer

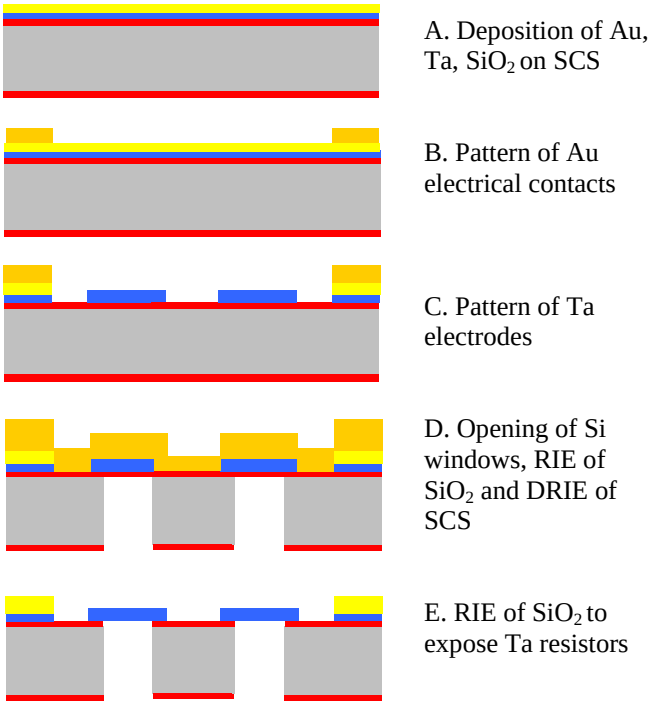

Figure 3: Fabrication sequence for the bubble generator

The three wafers were diced into 8 mm x 16 mm chips. The last step involved stacking the three separate layers, using a biocompatible ultraviolet-light-cured epoxy. The layers could also be anodically bonded. Once the three layers were bonded, the drugs were injected into the chip by breaking one of the membranes, dispensing the drugs using a syringe, and subsequently sealing the membrane using epoxy.

4 EXPERIMENTAL RESULTS

The devices were tested *in vitro* using a methylene blue dye, instead of vasopressin. The devices were placed inside of a small beaker filled with DI water and tested by applying an increasing dc- voltage and measuring the current. The device was optically inspected and recorded using a video camera connected to a stereoscope in order to register the conditions in which the ink is delivered. Figure 4 shows the I-V curve for generated bubbles using the heating elements. Bubbles were observed for an applied dc-voltage of 10 V and the measured current was approximately 330 mA. Fig. 5 shows the I-V curve for the hydrolysis configuration. Bubbles were observed for an applied dc-voltage of 15 V and the measured current was approximately 300 µA. Fig. 6 shows the blue solution jetted into the DI water using the heating elements.

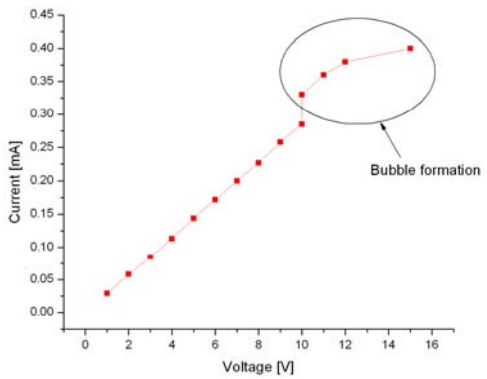

Figure 4: I-V curve for bubble generation using resistive configuration

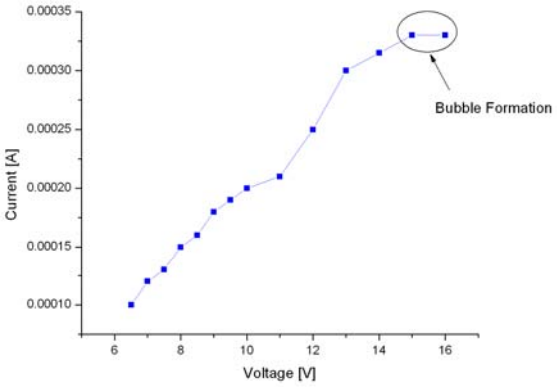

Figure 5: I-V curve for bubble generation using hydrolysis configuration

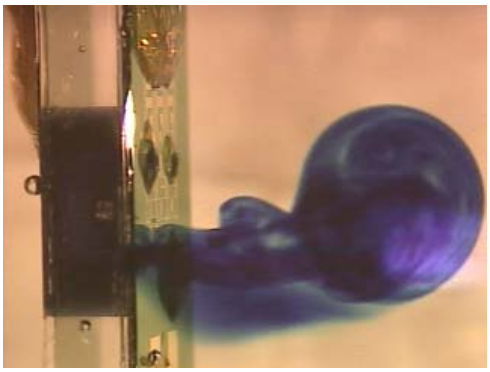

Figure 6: Test of drug-delivery system

5 DISCUSSION

The presented fabrication process allows the integration of three separate layers using a modular design. Each layer is fabricated independently, and subsequently stacked to form the miniaturized drug-delivery chip. One crucial aspect to note about the fabrication process is the chip hermeticity and biocompatibility, key requirements for implantable chips. The fabrication process for the membrane layer also provides a simple packaging solution, as the electrical routing is on the backside of the wafer, providing a seamless hermetic mechanical access to the reservoir chip for bubble formation. Bubbles were formed either using heating elements, or hydrolysis. Hydrolysis requires less power consumption than in the resistive configuration, as shown in Fig. 4 and Fig. 5, but the delivery rate was significantly lower. The resistive configuration also provides a more stable actuation voltage, unlike hydrolysis, which depends on the pH of the solution. Future work will focus on optimizing the heating elements in terms of material choice and geometry in order to reduce power consumption and further reduce the overall device dimensions. High pressure liquid chromatography analysis will be performed to verify that the drug composition is not affected by localized heating. The investigation will also be complemented by an ongoing animal study to determine the bioavailability of the drug using the device. Finally, the device will be integrated with electronics for wireless control and timed administration.

6 CONCLUSIONS

We presented the design, fabrication, preliminary experimental results for a novel drug delivery device for treating hemorrhagic shock on the battlefield. Current research focuses on improving power consumption, integrating sensors, and telemetry.

ACKNOWLEDGEMENTS

This work was made possible thanks to the support of the Army Research Office, through MIT's Institute for Soldier Nanotechnologies (ISN).

REFERENCES

[1] H. Wiggers and R. Ingraham, "Hemorrhagic shock: definition and criteria for its diagnosis," J Clin Invest, vol. 25, pp. 30-36, 1946.

[2] K. Okuyama, S. Mori, K. Sawa, and Y. Iida, "Dynamics of boiling succeeding spontaneous nucleation on a rapidly heated small surface," Int J Heat Mass Tran, vol. 49, pp. 2771-2780, 2006.

[3] C. Pang, Y. C. Tai, J. W. Burdick, and R. A. Andersen, "Electrolysis-based diaphragm actuators," Nanotechnology, vol. 17, pp. S64-S68, 2006.